

HIGHER ORDER HIERARCHICAL LEGENDRE BASIS FUNCTIONS APPLICATION TO THE ANALYSIS OF SCATTERING BY UNIAXIAL ANISOTROPIC OBJECTS

C. J. Lv, Y. Shi, and C. H. Liang

School of Electronic Engineering
Xidian University
Xi'an, Shanxi 710071, China

Abstract—An efficient technique for the analysis of scattering by uniaxial anisotropic objects is presented. The technique is based on the method of higher order MoM of the surface integral equations. This higher order MoM solution uses the higher order hierarchical basis functions which are based on the modified Legendre polynomials. Numerical results are given to demonstrate that the higher order hierarchical basis functions are more accurate and efficient in the calculations of uniaxial anisotropic objects scattering problem than the low-order basis function.

1. INTRODUCTION

The method of moments (MoM) is an efficient way to analyze the electromagnetic scattering problems formulated in terms of integral equations [1–3]. The conventional straightforward application of MoM involves low-order basis functions with the mesh cells' size in the order of one tenth of a wavelength, leading to a dense system of linear equations. With N being the number of unknowns, the memory requirement is $O(N^2)$, and the solution complexity is $O(N^3)$ for a direct solver and $O(N^2)$ for an iterative one. Several techniques have been proposed to reduce the memory demands as well as the solution complexity of the conventional MoM. Fast integral equation solvers, such as the multilevel fast multiple method (MLFMM) [4, 5], adaptive integral method (AIM) [6, 7] and its close counterpart, the precorrected FFT (PC-FFT) [8, 9], reach the solution complexity and memory

Corresponding author: C. J. Lv (02041377@163.com).

requirement as $O(N \log(N))$. However, when the scatter becomes electrically large, the number of unknowns becomes so large that even the fast integral equation solvers cannot solve it efficiently. Therefore, ways must be found to limit the number of unknowns.

We know that an efficient MoM technique should apply an iterative method. This requires a set of basis functions that do not lead to an ill-conditioned matrix. One of the most efficient ways is to employ higher order basis functions. However, the traditional higher order basis functions usually lead to an ill-conditioned system matrix. This problem can be avoided by making the basis functions near-orthogonal. In 2004, Jorgensen introduced a set of higher order hierarchical basis functions that provide a lower condition number than the existing higher order basis functions [10]. The basis is derived from orthogonal Legendre polynomials which are modified to impose continuity of vector quantities between neighboring elements while maintaining most of their desirable features. Moreover, a further improvement of the matrix condition number is obtained by defining appropriate scaling factors that multiply each basis function. As a result of the low condition number, MoM matrix systems with even tenth-order Legendre basis functions can be solved iteratively. These basis functions also have some other properties such as decreasing the number of unknowns, reducing the computational complexity in filling the impedance matrix, allowing different order bases used on different patches, etc.

Because of its good performance, a lot of scholars have solved many electromagnetic scattering problems using this kind of higher order basis functions [11–13]. However, there are few papers applying them to the anisotropic objects. In this paper, we will solve this problem using the higher order hierarchical Legendre basis functions.

2. FORMULATION

2.1. Higher Order Hierarchical Legendre Basis Functions

Here, we consider a curved quadrilateral patch of arbitrary order with an associated parametric curvilinear coordinate system defined by $-1 \leq u, v \leq 1$. The surface current on each patch can be represented as

$$\vec{J}_s = J_s^u \vec{a}_u + J_s^v \vec{a}_v \quad (1)$$

where \vec{a}_u and \vec{a}_v are the co-variant unitary vectors $\vec{a}_u = \partial \vec{r} / \partial u$ and $\vec{a}_v = \partial \vec{r} / \partial v$, J_s^u can be expanded as follows using higher order basis

functions.

$$J_s^u = \frac{1}{\zeta_s(u, v)} \sum_{m=0}^{M^u} \sum_{n=0}^{N^v} a_{mn}^u P_m(u) P_n(v) \quad (2)$$

where $\zeta_s(u, v) = |\vec{a}_u \times \vec{a}_v|$ is the surface Jacobian, and M^u and N^v denote the expansion order along the direction of the current and the transverse direction, respectively. a_{mn}^u are unknown coefficients, and $P_m(u)$ and $P_n(v)$ are expansion polynomials which are chosen as the Legendre polynomials

$$P_m(u) = \frac{1}{2^m m!} \frac{d^m}{du^m} (u^2 - 1)^m \quad (3)$$

The expansion in (2) is not appropriate if normal continuity of the current flowing across patch boundaries is to be enforced. Therefore, the polynomials need to be modified. In [10], the author presented the modified orthogonal Legendre polynomials, and J_s^u can be expanded as [10]

$$\begin{aligned} J_s^u(u, v) &= \frac{1}{\zeta_s(u, v)} \sum_{m=0}^{M^u} \sum_{n=0}^{N^v} b_{mn}^u \tilde{C}_m \tilde{P}_m(u) C_n P_n(v) \\ &= \frac{1}{\zeta_s(u, v)} \left\{ \sum_{n=0}^{N^v} [b_{0n}^u (1-u) + b_{1n}^u (1+u)] \tilde{C}_0 C_n P_n(v) \right. \\ &\quad \left. + \sum_{m=2}^{M^u} \sum_{n=0}^{N^v} b_{mn}^u \tilde{C}_m \tilde{P}_m(u) C_n P_n(v) \right\} \quad (4) \end{aligned}$$

where b_{mn}^u are the new unknown coefficients, and $\tilde{P}_m(u)$ is the alternative modified higher order polynomials

$$\tilde{P}_m(u) = \begin{cases} 1 - u, & m = 0 \\ 1 + u, & m = 1 \\ P_m(u) - P_{m-2}(u), & m \geq 2 \end{cases} \quad (5)$$

\tilde{C}_m and C_n are scaling factors which are chosen to make sure that the Euclidean norm of each function is in unity on a unit square patch.

$$\begin{aligned} \tilde{C}_m &= \begin{cases} \frac{\sqrt{3}}{4}, & m = 0, 1 \\ \frac{1}{2} \sqrt{\frac{(2m-3)(2m+1)}{2m-1}}, & m \geq 2 \end{cases} \quad (6) \\ C_n &= \sqrt{n + \frac{1}{2}} \end{aligned}$$

As for J_s^v , it can be obtained by interchanging u and v in (4). Thus, the surface current can be written as

$$\begin{aligned} \vec{J}_s = \frac{1}{\varsigma_s(u, v)} & \left(\vec{a}_u \sum_{m=0}^{M^u} \sum_{n=0}^{M^v-1} b_{mn}^u \tilde{C}_m \tilde{P}_m(u) C_n P_n(v) \right. \\ & \left. + \vec{a}_v \sum_{m=0}^{M^v} \sum_{n=0}^{M^u-1} b_{mn}^v \tilde{C}_m \tilde{P}_m(v) C_n P_n(u) \right) \end{aligned} \quad (7)$$

In the above equation, when $M^u = M^v = 1$, the well-known rooftop basis function can be obtained. For more information about the higher order basis functions, the reader can refer to [10]. In this paper, we will use the higher order hierarchical Legendre basis functions to analyze the scattering problems of anisotropic structure.

2.2. Integral Equations

For an interface of two dielectric objects, as shown in Figure 1, we use the well-known PMCHWT integral equations.

$$-\begin{bmatrix} \vec{E}^i \\ \vec{H}^i \end{bmatrix} = \int_{S'} \begin{bmatrix} \bar{\mathbf{G}}_e^1 + \bar{\mathbf{G}}_e^2 & \bar{\mathbf{G}}_{em}^1 + \bar{\mathbf{G}}_{em}^2 \\ \bar{\mathbf{G}}_{me}^1 + \bar{\mathbf{G}}_{me}^2 & \bar{\mathbf{G}}_m^1 + \bar{\mathbf{G}}_m^2 \end{bmatrix} \cdot \begin{bmatrix} \vec{J} \\ \vec{M} \end{bmatrix} d\vec{r}', \quad \vec{r} \in S \quad (8)$$

where \vec{E}^i and \vec{H}^i are the incident electromagnetic field. \vec{J} and \vec{M} are the surface electric and magnetic currents. $\bar{\mathbf{G}}_e^j$ and $\bar{\mathbf{G}}_{me}^j$ are the dyadic Green's functions in region j ($j = 1, 2$), corresponding to the electric

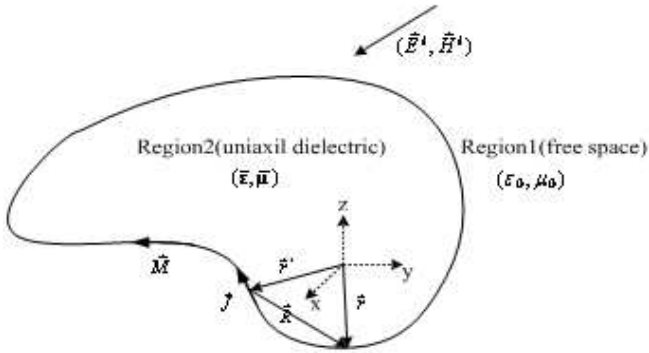


Figure 1. The geometry for the construction of PMCHWT formulations.

and magnetic fields due to delta electric current source. Likewise, $\bar{\mathbf{G}}_{\mathbf{em}}^j$ and $\bar{\mathbf{G}}_{\mathbf{m}}^j$ are associated with the electric and magnetic fields due to delta magnetic current source.

General uniaxial media are described by constitutive tensors of permittivity and permeability of the following form

$$\begin{aligned} \bar{\epsilon} &= \epsilon_{\perp} (\hat{a}\hat{a} + \hat{b}\hat{b}) + \epsilon_{//}\hat{c}\hat{c} = \epsilon_{\perp}\bar{\mathbf{I}} + (\epsilon_{//} - \epsilon_{\perp}) \hat{c}\hat{c} \\ \bar{\mu} &= \mu_{\perp} (\hat{a}\hat{a} + \hat{b}\hat{b}) + \mu_{//}\hat{c}\hat{c} = \mu_{\perp}\bar{\mathbf{I}} + (\mu_{//} - \mu_{\perp}) \hat{c}\hat{c} \end{aligned} \quad (9)$$

where $\bar{\mathbf{I}}$ is the unit dyadic. \hat{a} , \hat{b} and \hat{c} are the unit vectors. Without loss of generality it can be assumed that $\hat{c} = \hat{e}_z\epsilon_{//}$ is the relative permittivity along the distinguished axis (\hat{c} or $//$ axis), and ϵ_{\perp} is along the other directions (\hat{a} , \hat{b} or \perp axis). Similarly, $\mu_{//}$ and μ_{\perp} are the relative permeability along the $//$ and \perp axes. For nonmagnetic ($\bar{\mu} = \bar{\mathbf{I}}$) uniaxial dielectric media, the dyadic Green's functions take the form [14]

$$\begin{aligned} \bar{G}_e &= \frac{i\omega\mu_0}{4\pi} \left\{ \left[\frac{\nabla\nabla}{k_{\perp}^2} + \epsilon_{//}\bar{\epsilon}^{-1} \right] \frac{e^{ik_{\perp}R_e}}{R_e} - \left[\frac{\epsilon_{//}e^{ik_{\perp}R_e}}{\epsilon_{\perp}R_e} - \frac{e^{ik_{\perp}R}}{R} \right] \right. \\ &\quad \left[\frac{(\vec{R}\times\hat{c})(\vec{R}\times\hat{c})}{(\vec{R}\times\hat{c})^2} \right] - \left[\frac{\epsilon_{//}-\epsilon_{\perp}}{\epsilon_{\perp}} \frac{e^{ik_{\perp}(R_e+R)/2}}{R_e+R} \frac{\sin(k_{\perp}(R_e-R)/2)}{k_{\perp}(R_e-R)/2} \right] \\ &\quad \left. \left[\bar{\mathbf{I}} - \hat{c}\hat{c} - \frac{2(\vec{R}\times\hat{c})(\vec{R}\times\hat{c})}{(\vec{R}\times\hat{c})^2} \right] \right\} \end{aligned} \quad (10)$$

$$\begin{aligned} \bar{G}_m &= \frac{i\omega\epsilon_0}{4\pi} \left\{ \left[\frac{\nabla\nabla}{k_0^2} + \epsilon_{\perp}\bar{\mathbf{I}} \right] \frac{e^{ik_{\perp}R}}{R} + \left[\frac{\epsilon_{//}e^{ik_{\perp}R_e}}{R_e} - \frac{\epsilon_{\perp}e^{ik_{\perp}R}}{R} \right] \right. \\ &\quad \left[\frac{(\vec{R}\times\hat{c})(\vec{R}\times\hat{c})}{(\vec{R}\times\hat{c})^2} \right] + \left[(\epsilon_{//}-\epsilon_{\perp}) \frac{e^{ik_{\perp}(R_e+R)}}{R_e+R} \frac{\sin(k_{\perp}(R_e-R)/2)}{k_{\perp}(R_e-R)/2} \right] \\ &\quad \left. \left[\bar{\mathbf{I}} - \hat{c}\hat{c} - \frac{2(\vec{R}\times\hat{c})(\vec{R}\times\hat{c})}{(\vec{R}\times\hat{c})^2} \right] \right\} \end{aligned} \quad (11)$$

$$\begin{aligned}
\bar{G}_{me} = & \left(\frac{e^{ik_{\perp}R_e}}{4\pi R_e} - \frac{e^{ik_{\perp}R}}{4\pi R} \right) (\vec{R} \cdot \hat{c}) \\
& \left[\frac{(\vec{R} \times \hat{c}) [\hat{c} \times (\vec{R} \times \hat{c})] + [\hat{c} \times (\vec{R} \times \hat{c})] (\vec{R} \times \hat{c})}{(\vec{R} \times \hat{c})^4} \right] \\
& + (1 - ik_{\perp}R_e) \left(\frac{\varepsilon_{\parallel} e^{ik_{\perp}R_e}}{4\pi \varepsilon_{\perp} R_e^3} \right) \frac{(\vec{R} \times \hat{c}) [\vec{R} \times (\vec{R} \times \hat{c})]}{(\vec{R} \times \hat{c})^2} \\
& - (1 - ik_{\perp}R) \left(\frac{e^{ik_{\perp}R}}{4\pi R^3} \right) \frac{[\vec{R} \times (\vec{R} \times \hat{c})] (\vec{R} \times \hat{c})}{(\vec{R} \times \hat{c})^2} \quad (12)
\end{aligned}$$

$$\bar{G}_{em} = [\bar{G}_{me}]^T \quad (13)$$

where $\vec{R} = \vec{r} - \vec{r}'$, $R = |\vec{r} - \vec{r}'|$, $R_e = \sqrt{\varepsilon_{\parallel}(\vec{R} \cdot \vec{\varepsilon}^{-1} \cdot \vec{R})}$, $k_0 = \omega \sqrt{\mu_0 \varepsilon_0}$, $k_{\perp} = k_0 \sqrt{\varepsilon_{\perp}}$.

In (10)–(13), when $\vec{\varepsilon} = \vec{\mathbf{I}}$, the free space dyadic Green's functions can be obtained.

The surface currents in (8) can be expanded as

$$\vec{J} = \sum_{n=1}^N \alpha_n \vec{B}_n \quad \text{and} \quad \vec{M} = \sum_{n=1}^N \beta_n \vec{B}_n \quad (14)$$

where N is the total number of basis functions, and α_n and β_n are the unknown expansion coefficients. The basis functions \vec{B}_n take the form of (7). We can obtain the surface currents by solving (8). Then the scattering problem can be solved.

3. NUMERICAL RESULTS

In this section, we will present some numerical examples to validate the efficiency and accuracy of the higher order hierarchical Legendre basis functions and compare them with the roof-top basis function. Here, the GMRES iteration method with a relative error norm of 0.001 is adopted for all calculations. All calculations are carried out on a Pentium 4 with 2.8 G CPU and 1 GB RAM in single precision.

First, consider a uniaxial anisotropic dielectric cube with the edge length $2\lambda_0$, and λ_0 is the wave length in free space. Its relative permittivity is $\varepsilon_{\perp} = 5$, $\varepsilon_{\parallel} = 3$, and permeability is μ_0 in air. The

incident wave is given by $\vec{E}_{inc} = \vec{e}_x \exp(-jkz)$. As shown in Figure 2, the bistatic RCS with $\theta\theta$ -polarization obtained by the higher order MoM are compared with the results obtained by using the roof-top basis function and HFSS solution. A good agreement of the four results is observed. Table 1 gives several important parameters of the calculation. From Table 1, we can see that the two kinds of bases get the same results, but when the higher order basis functions are used, the number of unknowns decreases dramatically.

The second example is a conducting sphere coated with uniaxial anisotropic medium. The geometry of the structure is shown in Figure 3. The electric dimensions of the inner and outer radii are $k_0a_1 = 1.6\pi$ and $k_0a_2 = 2\pi$. The medium is TiO_2 whose relative permittivity is $\epsilon_t = 5.913$, $\epsilon_z = 7.197$, and permeability is μ_0 in air. With the same plane-wave source as that in the first example, the

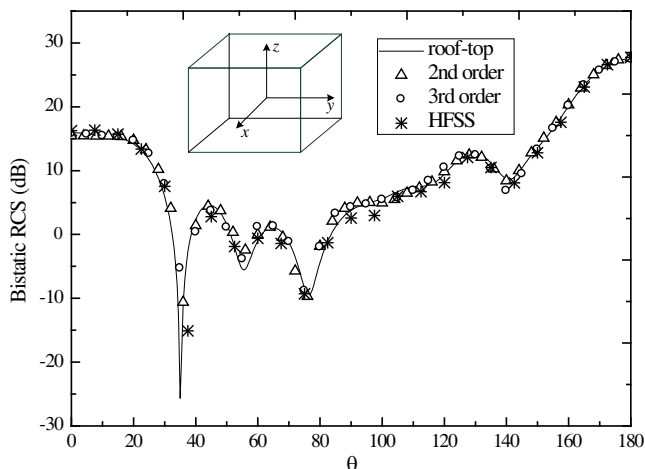


Figure 2. E plane bistatic RCS of the cube with edge length 2 m at 300 M.

Table 1. Several parameters in the calculation of the cube edge length 2 m.

Basis functions	1st order (roof-top)	2nd order	3rd order
Patch size (λ)	0.09	0.3	0.5
Patch number	3174	294	96
Unknowns	12696	4707	3456
Memory (MB)	1230	169	91

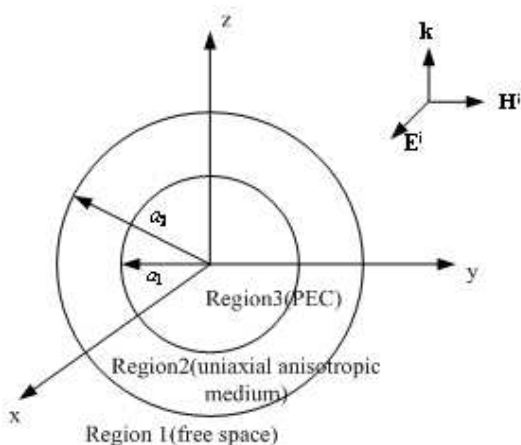


Figure 3. The geometry of scattering by a conducting sphere coated with uniaxial anisotropic medium.

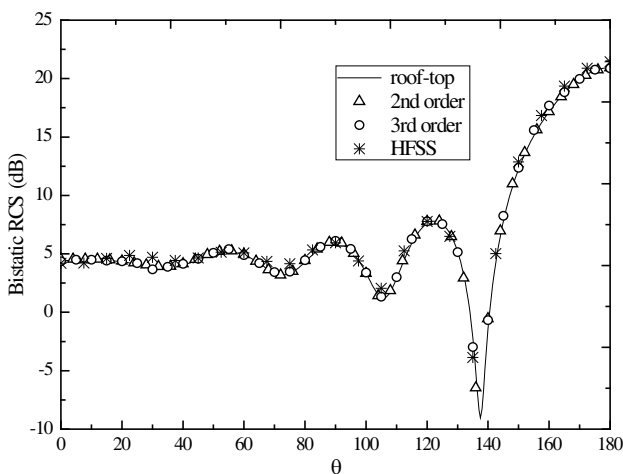


Figure 4. E plane Bistatic RCS of the uniaxial anisotropic medium coated sphere with radius $a_1 = 0.8$ m, $a_2 = 1$ m at 300 M.

bistatic RCS with $\theta\theta$ -polarization obtained by the higher order MoM are compared with the results obtained by using the roof-top basis functions and HFSS solution, as shown in Figure 4. Again, a good agreement of these results is observed. Several important parameters of the simulation are given in Table 2. From Table 2, we can see that

higher order basis functions require much fewer unknowns and less computer memory than low-order basis.

In order to show how the anisotropic permittivity influences the numerical result, we calculate two uniaxial anisotropic spheres. By comparing the anisotropic cases with isotropic case in Figure 5, we can see that the scattering characteristics of dielectric objects are greatly influenced by the presence of uniaxial anisotropy. By calculating other various uniaxial cases, we find that the RCS of a uniaxial anisotropic dielectric object is very sensitive to the anisotropy, even for a 1% variation of uniaxial anisotropy. But the uniaxial anisotropy influences the RCS in a complex fashion and is not predictable from a simple theory.

Table 2. Several parameters in the calculation of the uniaxial anisotropic medium coated sphere.

Basis functions	1st order (roof-top)	2nd order	3rd order
Patch size (λ)	0.1	0.32	0.55
Patch number	3106	366	208
Unknowns	9810	4528	2808
Memory (MB)	734	156	60

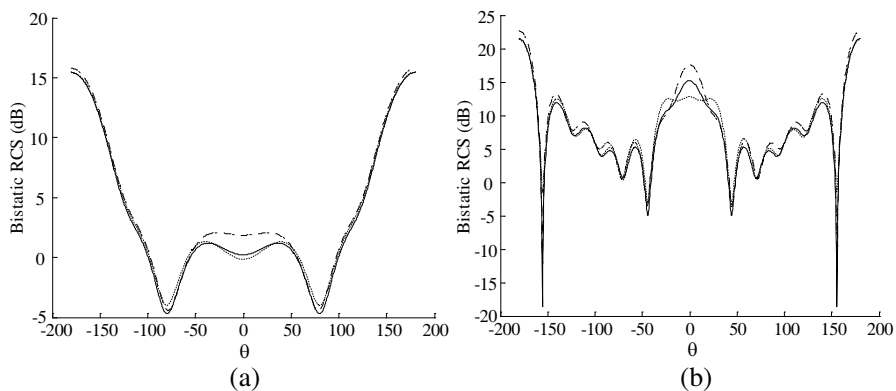


Figure 5. Bistatic RCS of the uniaxial anisotropic sphere and isotropic sphere (a) $k_0a = \pi$, (b) $k_0a = 2\pi$. Isotropic sphere — $\epsilon_{//} = \epsilon_{\perp} = 2.5$; Uniaxial anisotropic sphere ---- $\epsilon_{//} = 2.5, \epsilon_{\perp} = 2.4$, - - - - $\epsilon_{//} = 2.4, \epsilon_{\perp} = 2.5$.

4. CONCLUSION

A higher order MoM scheme has been presented for solving the scattering problem of the uniaxial anisotropic objects. Numerical examples for scattering by a PEC sphere coated with a uniaxial anisotropic medium and a uniaxial anisotropic dielectric cube demonstrate an excellent agreement between the results of our higher order MoM and the low-order MoM. It is shown that for electrically large scattering problem the higher order MoM yields a significant reduction of unknowns and thus decreases the computational demand dramatically. Therefore, it is efficient and accurate to use the higher order hierarchical MoM in the calculation of uniaxial anisotropic objects scattering problem. In the process of the calculation, we found that for the matrix filling time, higher order basis functions do not have an obvious advantage over low order basis functions. This is because our algorithm is not optimized. Therefore, our next work is improving the algorithm to decrease the matrix filling time.

ACKNOWLEDGMENT

This work is supported partly by the Program for New Century Excellent Talents in University of China and partially by the National Natural Science Foundation of China under Contract No. 60601028, No. 60801040, National Key Laboratory Foundation and the Fundamental Research Funds for the Central Universities.

REFERENCES

1. Harrington, R. F., *Field Computation by Moment Methods*, Wiley-IEEE, New York, 1993.
2. Rao, S. M., D. R. Wilton, and A. W. Glisson, "Electromagnetic scattering by surfaces of arbitrary shape," *IEEE Trans. Antennas Propag.*, Vol. 30, No. 3, 409–418, May 1982.
3. Schaubert, D. H., D. R. Wilton, and A. W. Glisson, "A tetrahedral modeling method for electromagnetic scattering by arbitrarily shaped inhomogeneous dielectric bodies," *IEEE Trans. Antennas Propag.*, Vol. 32, No. 1, 77–85, Jan. 1984.
4. Song, J. M., C. C. Lu, and W. C. Chew, "Multilevel fast multipole algorithm for electromagnetic scattering by large complex objects," *IEEE Trans. Antennas Propag.*, Vol. 45, No. 10, 1488–1493, Oct. 1997.
5. Sertel, K. and J. L. Volakis, "Multilevel fast multipole method

- solution of volume integral equations using parametric geometry modeling,” *IEEE Trans. Antennas Propag.*, Vol. 52, No. 7, 1686–1692, Jul. 2004.
6. Bleszynski, E., M. Bleszynski, and T. Jaroszewicz, “AIM: Adaptive integral method for solving large-scale electromagnetic scattering and radiation problems,” *Radio Science*, Vol. 31, No. 5, 1225–1251, Sep.–Oct. 1996.
 7. Zhang, Z. Q. and Q. H. Liu, “A volume adaptive integral method (VAIM) for 3-D inhomogeneous objects,” *IEEE Antennas Wireless Propag. Lett.*, Vol. 1, 102–105, 2002.
 8. Phillips, J. and J. White, “A precorrected-fft method for electrostatic analysis of complicated 3-d structures,” *IEEE Trans. Comput.-Aided Design Integr. Circuits Syst.*, Vol. 16, No. 10, 1059–1072, 1997.
 9. Nie, X. C., N. Yuan, L. W. Li, Y. B. Gan, and T. S. Yeo, “A fast volume-surface integral equation solver for scattering from composite conducting-dielectric objects,” *IEEE Trans. Antennas Propag.*, Vol. 53, No. 2, 818–824, Feb. 2005.
 10. Jorgensen, E., J. L. Volakis, P. Meincke, and O. Breinbjerg, “Higher order hierarchical legendre basis functions for electromagnetic modeling,” *IEEE Trans. Antennas Propag.*, Vol. 52, 2985–2995, Nov. 2004.
 11. Jorgensen, E., P. Meincke, and O. Breinbjerg, “A hybrid PO higher-order hierarchical MoM formulation using curvilinear geometry modeling,” *IEEE International Symposium on Antennas and Propagation*, Columbus, OH, USA, Jun. 2003.
 12. Jorgensen, E., O. Kim, P. Meincke, and O. Breinbjerg, “Higher-order hierarchical discretizationscheme for surface integral equations for layered media,” *IEEE Trans. on Geoscience and Remote Sensing*, Vol. 42, No. 4, 764–772, Apr. 2004.
 13. Kim, O. S., P. Meincke, O. Breinbjerg, and E. Jørgensen, “Method of moments solution of volume integral equations using higher-order hierarchical Legendre basis functions,” *Radio Science*, Vol. 39, 5003, 2004, 10.1029/2004RS003041.
 14. Weiglhofer, W. S., “Dyadic green’s functions for general uniaxial media,” *IEEE Proc. Microw. Antennas Propag.*, Vol. 137, No. 1, 5–10, Feb. 1990.